CHEMISTRY
A EUROPEAN JOURNAL

DOI: 10.1002/chem.200600208

Assembly of Nanotubes of Poly(4-vinylpyridine) and Poly(acrylic acid) through Hydrogen Bonding

Ying Tian, Qiang He, Yue Cui, Cheng Tao, and Junbai Li*[a]

Abstract: Nanotubes of poly(4-vinylpyridine) (PVP) and poly(acrylic acid) (PAA) were fabricated by hydrogen bonding based on layer-by-layer (LbL) assembly. The uniform and flexible tubular structures were characterized by scanning electron microscopy (SEM) and transmission electron microscopy (TEM). FTIR and X-ray photoelectron spectroscopy (XPS) measurements confirm the formation of hydrogen bonds in the assembled nanotubes. PAA can be released from the assembled PAA/PVP nanotubes in a basic aqueous solution to give the walls of the tubes a porous structure. Such assembled nanotubes can be considered as carriers for catalysts or drugs, especially in aqueous solution against capillary force.

Keywords: drug delivery · hydrogen bonds · layer-by-layer assembly · nanotubes · polymers

Introduction

Considerable attention has been paid to the preparation of various one-dimensional nanomaterials, because of their unique physicochemical properties and potential applications in various fields, such as electronics, optics, catalysis, and biological systems.[1–3] Most research has focused on the synthesis and functionalization of polymer nanotubes through the development of different approaches. A frequently used method is the template technique developed by Martin et al.,[4] in which highly ordered nanotube arrays can be obtained by using template membranes containing highly ordered pores.[5] A combination of self-assembly and the template technique is one of the most popular approaches.[6,7]

On the other hand, the novel layer-by-layer (LbL) assembly technique developed by Decher et al.[8,9] allows the fabrication of multilayer complex films on the planar substrates through the alternative deposition of oppositely charged polyelectrolytes in aqueous solution. This technique was applied by several groups for coating various particle surfaces as well as in constructing microcapsules.[10–12] Furthermore, uncharged driving forces, such as hydrogen bonds,[13] covalent bonds,[14] and ligand bonds,[15] have also been used to fabricate multilayer complex films, which clearly increases the area assembled by using the LbL assembly technique.

Recently, we developed the template-filter-pressure technique by combining the template technique and LbL assembly method, and used this to fabricate multicomponent nanotubes through electrostatic and covalent interactions.[16–18] In most cases, the sizes, shapes, and other structural properties of the assembled system can be well controlled by the pore structure obtained by using the template method.[19,20]

Herein, we use the template technique combined with the LbL assembly method to fabricate complex nanotubes through hydrogen bonding. The hydrogen-bonded LbL assembly was first introduced by Rubner and Zhang's groups, respectively.[21–23]

The advantage of the hydrogen-bonded LbL assembly is that it allows the fabrication of multilayer films in organic solvents. This is eventually impossible with electrostatic interactions, because a polycation and a polyanion will form a salt and precipitate in solution.[21] Strong interactions of the specific hydrogen-bonded polymers may enhance the stability of the assembled materials.

The assembled complex film of polyallylamine hydrochloride (PAH) and poly(acrylic acid) (PAA) can form a microporous structure upon exposure in solutions with different pH values.[24,25] Another reported system is the poly(4-vinylpyridine) (PVP) and PAA complex film, which is also sensitive to pH values. This film demonstrates that PAA can be dissolved out from the multilayer films in a basic solution

[a] Dr. Y. Tian, Dr. Q. He, Dr. Y. Cui, Dr. C. Tao, Prof. Dr. J. Li
Beijing National Laboratory for Molecular Sciences, Key Lab of Colloid and Interface Science, Center for Molecular Sciences
Institute of Chemistry, Chinese Academy of Sciences
Zhong Guan Cun, Beijing 100080 (China)
Fax: (+86) 10-8261-2629
E-mail: jbli@iccas.ac.cn

to produce pore structures without destroying the framework of the film.[26,27] Sukhishvili et al. prepared erasable hydrogen-bonded multilayers containing weak polyacids, which could be assembled at low pH values and subsequently dissolved at higher pH values.[28,29] With this feature, one could consider constructing a new type of porous polymer complex film with potential applications in many fields, such as biology and medicine.[28,30]

In this study, we used PVP and PAA as hydrogen acceptor and donor, respectively, to prepare multilayer complex nanotubes via a hydrogen-bonded LbL assembly in an organic solvent. The structural changes in these assembled nanotubes were also investigated in a basic aqueous solution. Due to the low solubility of PVP in the basic solution, it remains in the substrate. Thus, the porous structures in the wall of the assembled nanotubes are formed.

Results and Discussion

Results of UV spectroscopy show the growth process of the multilayer assembly of PVP and PAA obtained by performing the LbL technique on a quartz slide. Figure 1A shows the UV absorption spectra of the assembled PAA/PVP film containing different numbers of layers. To increase the detected intensity we measured the UV absorption spectrum after the assembly of every four layers. Thus, a total of 12 measurements were taken for the total of 48 assembled layers. The feature absorption band at 256 nm represents the contribution of pyridine from the PVP layers. Figure 1B shows that the UV absorbance of the assembled complex films at 256 nm increases linearly as the number of layers increases, indicating that there is an approximately equal deposition of PAA and PVP in each adsorption process.

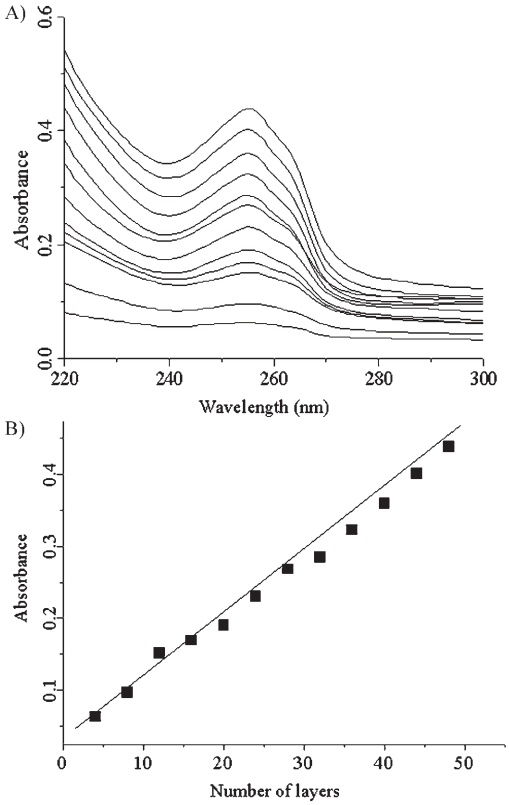

Figure 1. A) UV spectra of $(PAA/PVP)_n$ multilayer films, in which $n = 4$–48, assembled on a quartz substrate. The spectra were obtained after every four cycles of assembly. B) Feature absorbance of pyridine from PVP at 256 nm versus the number of layers deposited.

Scanning electron microscopy (SEM) images (Figure 2A) show that the assembled $(PAA/PVP)_5$ possesses a typically tubular structure. The regular $(PAA/PVP)_5$ array exhibits

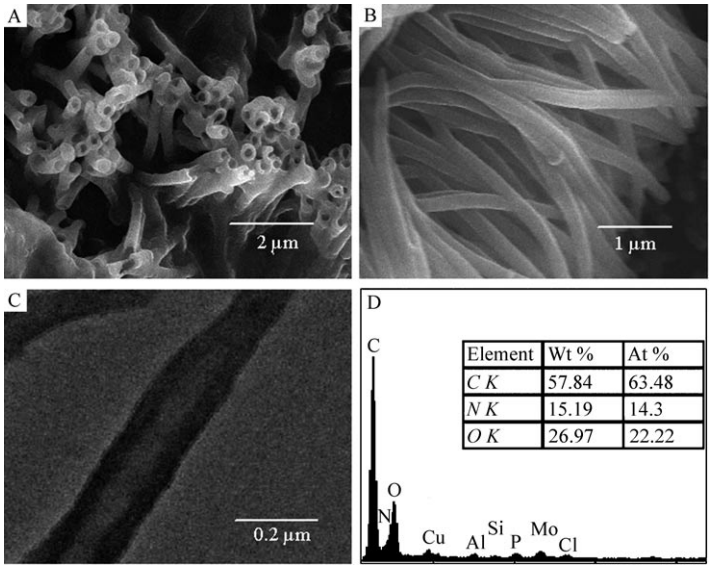

Figure 2. A) and B) SEM images of assembled $(PAA/PVP)_5$ nanotubes at different magnitudes. C) TEM image of a single $(PAA/PVP)_5$ nanotube. D) EDX analysis of a $(PAA/PVP)_5$ nanotube.

tubes with smooth and clean surfaces, a wall thickness of around 50 ± 5 nm, and lengths in the order of the thickness of a polycarbonate (PC) membrane (ca. 13 μm). The fabricated $(PAA/PVP)_5$ nanotubes exhibit a good stability and flexibility (Figure 2B). The tube diameter is controlled by the pore size as well as the assembled layers. The transmission electron microscopy (TEM) image in Figure 2C demonstrates further the tubular structure and provides information on the wall thickness, approximately 50 nm, which is similar to that estimated by SEM. Figure 2D displays the energy-dispersive X-ray (EDX) spectra. The main elements of carbon, nitrogen, and oxygen (hydrogen excepted) are detected, indicating that the expected composites from PAA and PVP are exiting from the tubes.

The formation of hydrogen bonds between the two polymers was confirmed by recording FTIR spectra (Figure 3A). The broad absorption band of PAA at around 3000 cm^{-1} and the peak at 1710 cm^{-1} are assigned to vibrations of the carbonyl function of carboxylic acid groups in the associated state.[15] The peaks appearing at 1597, 1555, and 1452 cm^{-1}

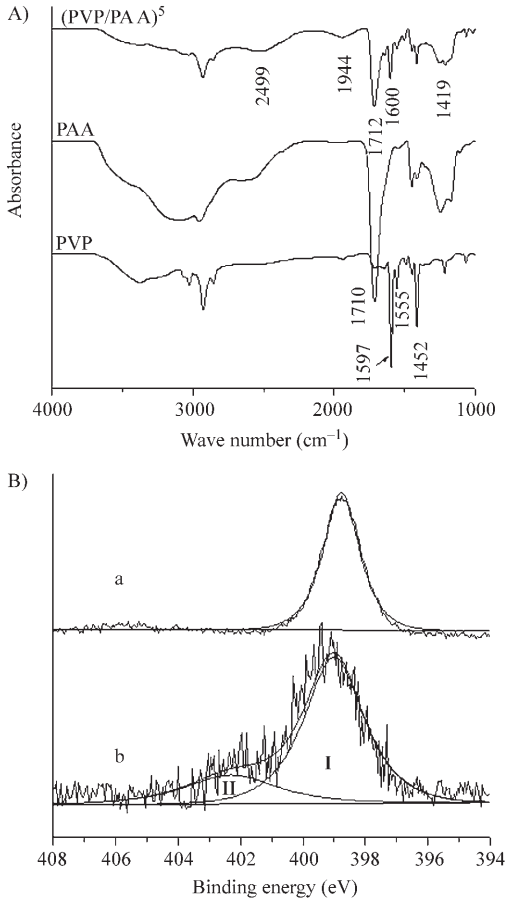

Figure 3. A) FTIR spectrum of $(PAA/PVP)_5$ nanotubes on a CaF_2 substrate compared with pure PAA and PVP films. B) Nitrogen (1s) XPS spectra of $(PAA/PVP)_5$ nanotubes (curve b) and pure PVP film (curve a).

are attributed to the ring vibration of the pyridine of PVP. Figure 3A also shows the IR spectrum of five-bilayer $(PVP/PAA)_5$ nanotubes. A C=O stretching vibration appeared at 1712 cm^{-1}, revealing that the carbonyl group is in a less-associated state than that in pure PAA. A clear O–H stretching vibration appeared at 2499, and the peak at 1944 cm^{-1} demonstrates that the hydroxyl group is formed through hydrogen bonds within PAA and PVP rather than by the formation of the weak inner hydrogen bond in pure PAA. This proves that the assembled PAA/PVP nanotubes are constructed through hydrogen bonds. No significant changes are found in the band positions from 1100 to 1700 cm^{-1} in the assembled nanotubes, in contrast to those of the pure PAA or PVP film within the same range. These results provide further evidence that the assembled PAA/PVP nanotubes are formed through hydrogen bonding rather than through electrostatic attraction. X-ray photoelectron spectroscopy (XPS) was used to detect the compositions of the nanotubes (Figure 3B). The peak of N1s appeared at 398.5 eV (curve a), which represents the contribution of the pyridine nitrogen of pure PVP film.[12] However, the absorption of N1s obtained in the assembled $(PAA/PVP)_5$ nanotubes appears as two peaks (curve b). One is at 399 eV (zone I), which can be ascribed to the contribution of a nitrogen atom from PVP. Another peak located at 403 eV (zone II) indicates a nitrogen atom that has a new chemical environment. The increase in binding energy means that the partial nitrogen in the assembled $(PAA/PVP)_5$ has been occupied by a newly formed hydrogen bond. At this stage, some nitrogen atoms in the pyridine ring serve as electron donors for the formation of the hydrogen bond.

As the number of assembled PAA/PVP layers increases, the wall thickness of the complex tubes obtained should increase. Figure 4A shows the SEM image of the nanotubes

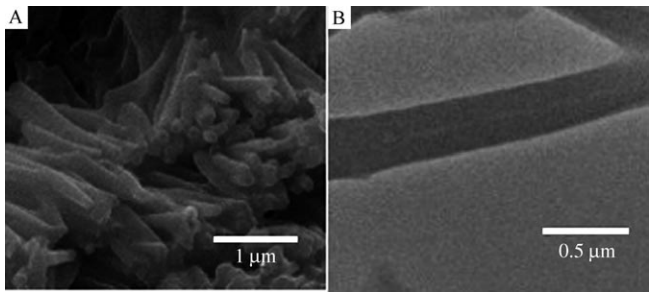

Figure 4. A) SEM image of $(PAA/PVP)_{10}$ nanotubes. B) TEM image of a $(PAA/PVP)_{10}$ nanotube.

obtained by assembling ten bilayers of PAA/PVP within the pores of the PC template. The tubular channel becomes smaller and is hardly observed. The TEM image of the $(PAA/PVP)_{10}$ nanotubes in Figure 4B proves that the wall thickness of the nanotubes increases to about 80 ± 10 nm (estimated from a nonuniform tube), which is clearly thicker than that of the $(PAA/PVP)_5$ nanotubes. Therefore, the wall thickness of the assembled nanotubes does indeed increase as the number of assembled layers increases. The thickness of each bilayer estimated roughly from the wall thickness of $(PAA/PVP)_5$ nanotubes is about 10 nm, and the value obtained from the $(PAA/PVP)_{10}$ nanotubes is approximately 8 nm. The estimated bilayer thickness is in the same order and is definitely consistent. However, relative to the theoretical values calculated from the chemical structure, the estimated thickness is still large. This can be ascribed to the effect of the residual materials that are not removed from the wall. Nevertheless, even accounting for the errors, we can still deduce that the wall thickness of the assembled nanotubes increases as the cycle number increases, and is to some degree controllable.

As reported by Zhang and co-workers, PAA can be released from the assembled complex film of $(PAA/PVP)_n$, in which n is the number of deposition cycles, if the film is immersed in a more basic solution. To prove this, we deposited the assembled $(PAA/PVP)_5$ nanotubes in an aqueous NaOH solution of pH 11 for 10 min, then removed the samples and rinsed them with water in preparation for the XPS measurements. Figure 5 shows the variation in composition of the assembled $(PAA/PVP)_5$ nanotubes before (curve A) and after

(curve B) immersion in the NaOH solution. The main peaks observed are those of C1s at 285 eV (curves A and B). Curve A demonstrates that before the nanotubes were immersed in the NaOH solution, a weak peak appeared at 291 eV, corresponding to the carbon atom of carboxylic acid in PAA, which was also reported by Zhang.[26] After immersion, the weak peak disappeared, indicating that PAA was removed from the assembled nanotubes by the basic aqueous solution. To demonstrate further that PVP remains in the framework after immersion, we performed AFM. Figure 6 displays the height and deflection AFM images of the assembled $(PAA/PVP)_5$ nanotubes before and after etching with the basic solution. Figure 6A represents the assembled tube before immersion, showing the clearly tubular structure with a relatively smooth surface. Figure 6B represents the tube after immersion, indicating the porous structure within the tube wall. The pore size was estimated roughly from the enlarged insert image of Figure 6B to be about 50 nm. These results demonstrate further the release of PAA from the assembled $(PAA/PVP)_5$ nanotubes.

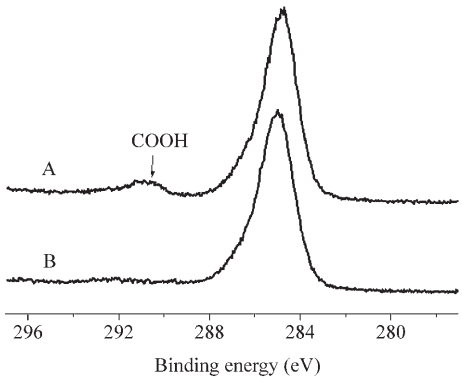

Figure 5. Carbon (1s) XPS spectra of $(PAA/PVP)_5$ assembled nanotubes before (A) and after (B) immersing in NaOH aqueous solution (pH 11) for 5 min.

Figure 7 shows HRTEM images of the assembled $(PAA/PVP)_5$ nanotubes before (A) and after (B) treatment with basic solution. Figure 7A shows the tubular structure with a nonporous wall, however, as the tubes were immersed in a NaOH solution of pH 11 for 10 min, pores in the wall could be observed (Figure 7B). This proves that PAA is released from the assembled $(PAA/PVP)_5$ nanotubes and that PVP remains in the wall to serve as the framework of the tubes.

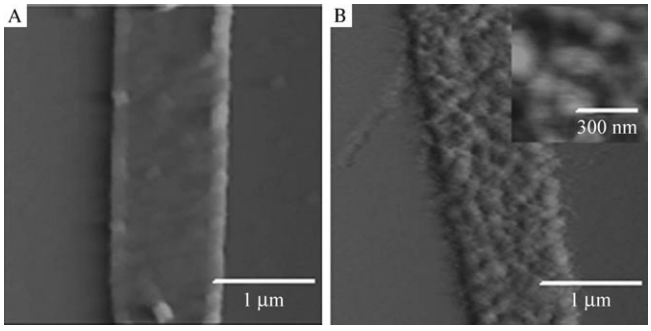

Figure 6. Height and deflection AFM images (3 μm × 3 μm) of $(PAA/PVP)_5$ LbL-assembled nanotubes before (A) and after (B) immersing in NaOH aqueous solution. The insert image (700 nm × 700 nm) shows the pores within the nanotube wall.

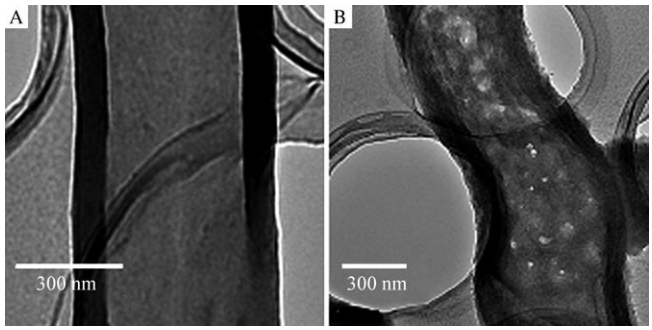

Figure 7. HRTEM images of $(PAA/PVP)_5$ LbL-assembled nanotubes before (A) and after (B) immersing in NaOH aqueous solution.

Conclusion

We have demonstrated that PAA and PVP can be fabricated into nanotubes through hydrogen bonding within the wall of template pores. The assembled nanotubes have a uniform size and flexible shape. The wall thickness of the nanotubes depends strongly on the number of PAA/PVP pairs assembled. To some extent, the wall thickness is controllable. Results of FTIR and XPS analysis determined the composition of the assembled nanotubes and confirmed the formation of hydrogen bonds within the tubes. We also proved that PAA can be released from the assembled nanotubes under strongly basic conditions. Such assembled nanotubes with porous walls may be applied as carriers of catalysts and drugs to achieve a better dispersion and diffusion of species, especially in an aqueous system.

Experimental Section

Materials: Polycarbonate (PC) membranes with a pore diameter of 200 nm and a membrane thickness of 13 μm were obtained from Whatman. Poly(4-vinylpyridine) (PVP, $M_r = 60000$) obtained from Sigma-Aldrich and poly(acrylic acid) (PAA, $M_r = 135{,}000$, 25 % solution in water) purchased from ACROS were used without further treatment. PVP and PAA were prepared as 0.05 wt % methanol solutions.

Methods: The NH_2-terminated quartz substrate was first immersed in a PVP/methanol solution for 10 min. The slide was then rinsed with methanol and dried under nitrogen. Next, the slide was transferred into a PAA/methanol solution for 10 min. The multilayer film is expressed as $(PAA/PVP)_n$, in which n is the number of deposition cycles. For the preparation of complex nanotubes, the PC membrane was first coated with PAA by filtering the PAA solution through the pores of the membrane. Then the PVP solution was deposited in the template pores and interacted with PAA through hydrogen bonding. After several cycles, multilayer films were formed on the inner walls of the PC membrane pores. Finally, the

films deposited on the top and bottom surfaces of the membrane were removed by wiping the surfaces with filter paper. Once the PC membrane was dissolved by dichloromethane, the nanotubes were liberated into the solution. The assembly procedure is depicted in Scheme 1.

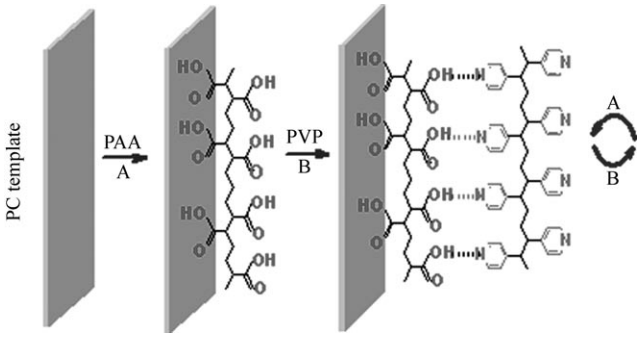

Scheme 1. Assembly of PAA/PVP nanotubes within the walls of the PC template by means of the LbL technique based on hydrogen bonding.

Characterizations: The quartz slide and CaF_2 plate were used for UV/Vis analysis and FTIR spectroscopy measurements, respectively. Both surfaces of quartz and CaF_2 were modified with a precursor layer of polyethyleneimine (PEI). FTIR spectra were recorded by using a TENSOR 27 instrument (BRUKER, Germany). The UV/Vis spectra were recorded by using a HITACHI U-3010 UV/Vis spectrometer. The SEM micrographs were acquired by using an S-4300 apparatus (HITACHI, Japan) and TEM was performed by using a 200-CX microscope (JEM, Japan). HRTEM images were obtained by using a Philips CM200-FEG instrument.

Acknowledgements

This work was supported financially by the National Nature Science Foundation of China (project nos. 20404015 and 20471063) and the Chinese Academy of Sciences.

[1] J. Cioslowski, N. Rao, D. Moncrieff, *J. Am. Chem. Soc.* **2002**, *124*, 8485.
[2] V. Percec, M. Flodde, T. K. Bera, Y. Miura, I. Shiyangovskaya, A. Rapp, H. W. Spiess, S. D. Hudson, H. Duan, *Nature* **2002**, *419*, 384.
[3] J. K. J. Knapen, A. W. van der Made, J. C. de Wilde, P. W. N. M. van Leeuwen, P. Wijkens, D. M. Frove, G. van Koten, *Nature* **1994**, *372*, 659.
[4] H. Masuda, K. Fukuda, *Science* **1995**, *268*, 1466.
[5] G. Sauer, G. Brehm, S. Schneider, K. Nielsch, R. B. Wehrspohn, J. Choi, H. Hofmeister, U. Gosele, *J. Appl. Phys.* **2002**, *91*, 3243.
[6] S. F. Hou, C. C. Harrell, L. Trofin, P. Kohli, C. R. Martin, *J. Am. Chem. Soc.* **2004**, *126*, 5674.
[7] L. Y. Zhao, W. S. Yang, Y. Luo, T. Y. Zhai, G. J. Zhang, J. N. Yao, *Chem. Eur. J.* **2005**, *11*, 3773.
[8] G. Decher, J. Hong, *Makromol. Chem. Macromol. Symp.* **1991**, *46*, 321.
[9] G. Decher, *Science* **1997**, *277*, 1232.
[10] Y. Wang, A. Yu, F. Caruso, *Angew. Chem.* **2005**, *117*, 2948; *Angew. Chem. Int. Ed.* **2005**, *44*, 2888.
[11] R. Heuberger, G. Sukhorukov, J. Vörös, M. Textor, H. Möhwald, *Adv. Funct. Mater.* **2005**, *15*, 357.
[12] Z. An, C. Tao, G. Lu, H. Möhwald, S. Zheng, Y. Cui, J. Li, *Chem. Mater.* **2005**, *17*, 2514.
[13] S. Y. Yang, D. Lee, R. E. Cohen, M. F. Rubner, *Langmuir* **2004**, *20*, 5978.
[14] Y. Zhang, S. Yang, Y. Guan, W. Cao, J. Xu, *Macromolecules* **2003**, *36*, 4238.
[15] M. Wanunu, R. Popovitz-Biro, H. Cohen, A. Vaskevich, I. Rubinstein, *J. Am. Chem. Soc.* **2005**, *127*, 9207.
[16] S. F. Ai, G. Lu, Q. He, J. B. Li, *J. Am. Chem. Soc.* **2003**, *125*, 11140.
[17] Y. Tian, Q. He, C. Tao, J. B. Li, *Langmuir* **2006**, *22*, 360.
[18] S. F. Ai, Q. He, C. Tao, S. P. Zheng, J. B. Li, *Macromol. Rapid Commun.* **2005**, *26*, 1965.
[19] J. E. Meegan, A. Aggeli, N. Boden, R. Brydson, A. P. Brown, L. Carrick, A. R. Brough, A. Hussain, R. J. Ansell, *Adv. Funct. Mater.* **2004**, *14*, 31.
[20] Z. J. Liang, A. S. Susha, A. Yu, F. Caruso, *Adv. Mater.* **2003**, *15*, 1849.
[21] W. B. Stockton, M. F. Rubner, *Macromolecules* **1997**, *30*, 2717.
[22] L. Y. Wang, Z. Q. Wang, X. Zhang, J. C. Shen, L. F. Chi, H. Fuchs, *Macromol. Rapid Commun.* **1997**, *18*, 509.
[23] L. Y. Wang, Y. Fu, Z. Q. Wang, Y. G. Fan, X. Zhang, *Langmuir* **1999**, *15*, 1360.
[24] J. D. Mendelsohn, C. J. Barrett, V. V. Chan, A. J. Pal, A. M. Mayes, M. F. Rubner, *Langmuir* **2000**, *16*, 5017.
[25] Q. Li, J. F. Quinn, F. Caruso, *Adv. Mater.* **2005**, *17*, 2058.
[26] Y. Fu, S. L. Bai, S. X. Cui, D. L. Qiu, Z. Q. Wang, X. Zhang, *Macromolecules* **2002**, *35*, 9451.
[27] H. Y. Zhang, Y. Fu, D, Wang, L. Y. Wang, Z. Q. Wang, X. Zhang, *Langmuir* **2003**, *19*, 8497.
[28] V. Kharlampieva, S. A. Sukhishvili, *Macromolecules* **2002**, *35*, 301.
[29] S. A. Sukhishvili, S. Granick, *J. Am. Chem. Soc.* **2000**, *122*, 9550.
[30] Y. J. Zhang, Y. Guan, S. G. Yang, J. Xu, C. C. Han, *Adv. Mater.* **2003**, *15*, 832.

Received: February 14, 2006
Published online: April 10, 2006

